Proceedings of ICRC 2001: 4003 © Copernicus Gesellschaft 2001

ICRC 2001

Splash and reentrant albedo observations of electrons and positrons at a 4.2 GV vertical magnetic cutoff

M. A. DuVernois[1,*], A. S. Beach[1], J. J. Beatty[1], A. Bhattacharyya[2], C. Bower[2], S. Coutu[1], A. W. Labrador[3], S. P. McKee[4], S. Minnick[1], D. Müller[3], J. Musser[2], S. Nutter[1,], M. Schubnell[4], S. Swordy[3], G. Tarlé[4], and A. Tomasch[4]**

[1]Department of Physics, Pennsylvania State University, University Park, PA (USA)
[2]Department of Physics, Indiana University, Bloomington, IN (USA)
[3]Enrico Fermi Institute & Department of Physics, Unversity of Chicago, Chicago, IL (USA)
[4]Department of Physics, University of Michigan, Ann Arbor, MI (USA)
[*]Now at the School of Physics & Astronomy, University of Minnesota, Minneapolis, MN (USA)
[**]Now at the Department of Physics & Geology, Northern Kentucky University, Highland Heights, KY (USA)

Abstract. The HEAT-$\overline{p}$ balloon magnet spectrometer was used to measure the rigidity spectra of splash and reentrant albedo particles. Although the primary objective of the HEAT-$\overline{p}$ instrument is the measurement of antiproton abundances at high energy, a large sample of events below local geomagnetic cutoff was also collected. The top-bottom symmetry of the detector configuration and the excellent particle identification required for antiproton measurements allowed for clean measurements of the upward and downward-going electron and positron albedos. These measurements are important in understanding the detailed properties and model dependencies of both the Earth's magnetosphere and of extensive air showers at small atmospheric depths.

1 Introduction

Electrons and positrons in the Galaxy have a unique propagation history, distinct from the more abundant hadronic cosmic rays. Therefore, the electrons are important trackers for probing the propagation of all cosmic rays within the Galaxy. Within the atmosphere, at balloon altitudes, the measurement of primary electrons and positrons is complicated by the presence of secondary electrons and positrons largely produced by hadronic interactions of the nuclear component of the cosmic rays with the atmosphere. Primary protons and heavy nuclei interact in the atmosphere to produce short-lived pions and kaons. Electrons (both positrons and negative electrons) are among the decay products of the short-lived species. Secondary electrons and positrons are produced in roughly equal numbers through decay chains such as the $\pi^{\pm} \rightarrow \mu^{\pm} \rightarrow e^{\pm}$ reactions.

Below local geomagnetic cutoff, the electrons at balloon altitudes include an upward-going particle population (the splash albedo) and a downward-traveling particle population (the reentrant albedo). The splash electron albedo particles are produced largely by incident protons at large zenith angles. The reentrant electron albedo then consists of the splash albedo population after propagation back to the top of the atmosphere and along the trapping magnetic field lines to the field-conjugate location on the opposite side of the Earth. Simulations and balloon measurements have both been performed to track the production and propagation processes of the albedo populations.

The High-Energy Antimatter Telescope (HEAT) in its antiproton ($\overline{p}$) configuration was designed to measure antiprotons up to 50 GeV in energy and was flown from Fort Sumner, New Mexico, in 1999 and 2000. The instrument is top-to-bottom symmetric with time-of-flight (ToF) scintillator paddles at the extremes, 140 layers of multiple-dE/dx wire chambers split equally above and below the 1 Tesla superconducting magnet with a 479 channel drift-tube-hodoscope (DTH) for tracking in the central field. The instrument is described fully elsewhere (Bower *et al.* 1999 and Nutter *et al.* 2001).

During the 2000 New Mexico flight analyzed here, the instrument flew at a nearly constant 4.2 GV vertical geomagnetic cutoff rigidity allowing measurements significantly below cutoff. Although the instrument was optimized for antiprotons, a significant sample of electrons was also measured.

2 Data analysis

To distinguish the reentrant albedo population from the atmospheric secondaries below geomagnetic cutoff, the intensity of electrons is examined as a function of depth in the atmosphere. During the course of the flight, the residual atmosphere above the instrument (the overburden) varied between about 4 and 10 g/cm^2. The flight was divided into periods corresponding to six different depth levels. Note that the minimum and maximum atmospheric depths have the greatest statistics.

Electrons and positrons are selected in the data by applying the following selection criteria:

Correspondence to: M. A. DuVernois
(duvernoi@physics.umn.edu)

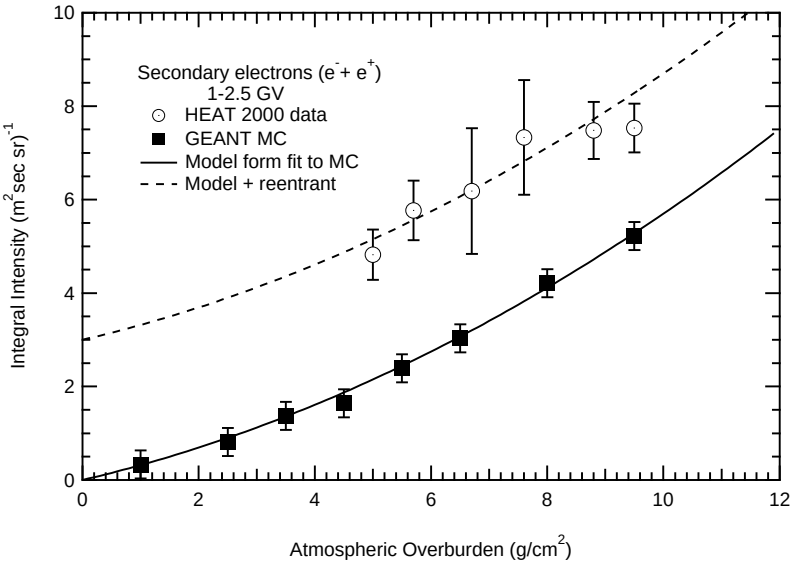

Fig. 1. Atmospheric growth curve for secondary electrons with rigidity 1–2.5 GV (well below geomagnetic cutoff). HEAT data is shown as open circles and the GEANT-based atmospheric simulation as closed squares. HEAT errors are statistical while GEANT errors are an estimate of the uncertainty of the atmospheric model combined with statistics. The solid curve is a two component exponential fit to the GEANT results. The dashed curve is the same curve with an offset at zero atmospheric overburden chosen to fit the HEAT flight data. This offset is the reentrant electron albedo.

– downward-going for reentrant & atmospheric secondaries (ToF)

– upward-going for splash (ToF)

– charge measured in the scintillators consistent with Z=1 (ToF)

– good track in the DTH

– rigidity selection for 1–4 GV (DTH)

– energy-losses in the dE/dx consistent with $e^{\pm}$

– a relativistic ToF measurement ($\beta > 0.8$) to distinguish positrons from the background protons.

¿From this clean sample of low-rigidity electrons and positrons, the absolute intensity of the total electron population (e^+ + e^-) is determined for the six depth levels. A full determination of the geometrical factors, efficiencies, and live time for this flight have not yet been performed, so a provisional acceptance is taken to normalize the HEAT-$\overline{p}$ splash albedo at 1–2.5 GV with the HEAT-$e^{\pm}$ splash albedo at the same rigidity range.

3 Magnetospheric physics

3.1 Reentrant electron albedo

The growth curve of electrons (electron intensity as a function of atmospheric depth) is shown in Figure 1. The excursions to deeper depth (near 10 g/cm^2) were due to the overflight of cirrus clouds during the balloon flight.

A Monte Carlo (MC) simulation of the atmosphere using the CERN detector, simulation, and hadronic interaction tools (GEANT and FLUKA) are compared with the HEAT data below geomagnetic cutoff (Fassó *et al.* 1993 and Brun *et al.* 1994). The results shown in Figure 1 (as the solid squares) are the integrated MC contributions in the 1–2.5 GV rigidity bin from secondary particles produced from primary protons and scaled to account for heavier nuclei. The curve is a double exponential fit to the MC simulation points.

Electron events above the level of secondary production are attributed to reentrant albedo particles. An extrapolation of the flight growth curve to zero g/cm^2 provides an estimate of the intensity of the reentrant electron albedo at the top of the atmosphere (ToA). The error is based on the statistics of the measurement, the systematics of the growth curve fit, and the systematics from requiring the splash albedo intensities from HEAT-$e^{\pm}$ and HEAT-$\overline{p}$ to agree. Possible systematics in the GEANT-based atmospheric simulation are not estimated due to considerable uncertainty in secondary particle generation in the atmosphere.

This new measurement is divided into two bins (1–2.5 GV and 2.5–4 GV) and is plotted with filled circles along with previous observations of the reentrant electron albedo on Figure 2. The previous HEAT result (Barwick *et al.* 1998) is immediately to the right of the lower energy current data point and in good agreement. The observations of Verma (1967) and Israel (1969) were obtained at Palestine, Texas, where the vertical cutoff is similar (4.5 GV). The HEAT measurements are consistent with a smooth extrapolation from the Israel (1969) datum, the Schmoker and Earl (1965) and Stephens (1970) upper limits, and the measurements at lower geomagnetic cutoff from Rockstroh & Webber (1969) and Hovestadt *et al.* (1971). The Verma (1967) measurements, however, show a significantly higher intensity than did Israel (1969)—secondary production calculations were similar for the two experiments, so this is a measured difference and not a difference in background subtraction.

Theoretical modeling of the reentrant albedo has not been significant, although Treiman (1953), Ray (1962), and Konig (1981) have addressed the basic physics. With the recent

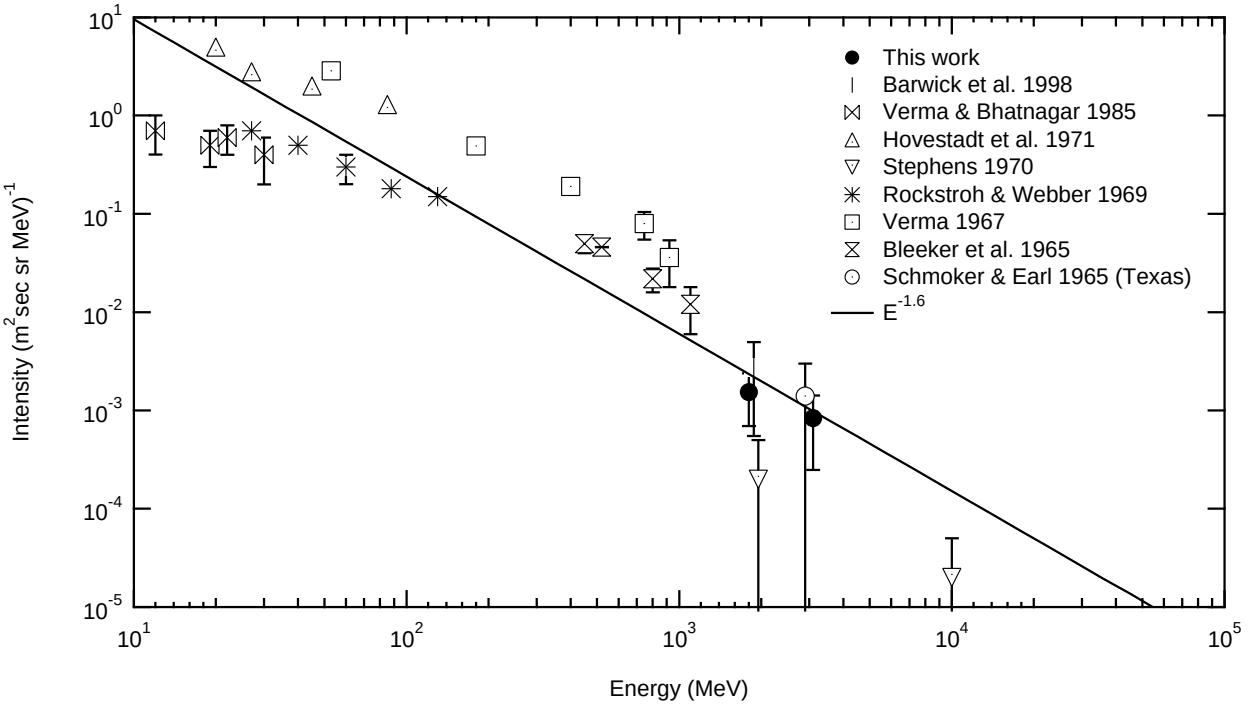

Fig. 2. Reentrant electron albedo fluxes from a variety of different experiments from the mid-1960s through the previous HEAT experiment (Barwick et al. 1997) and the current data. The $E^{-1.6}$ spectra is to guide the eye—theoretical modeling for the reentrant electron albedo flux predicts a complex form (not a simple power-law). (Schmoker & Earl data is from the Texas flight and not the Minnesota flight.)

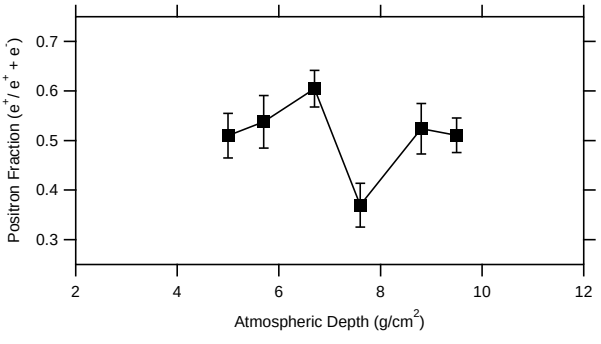

Fig. 3. Positron fraction in the albedo (splash + reentrant). Secondary production processes in the atmosphere give a positron fraction of close to 0.5. Propagation through the magnetosphere and corresponding energy losses should not change this.

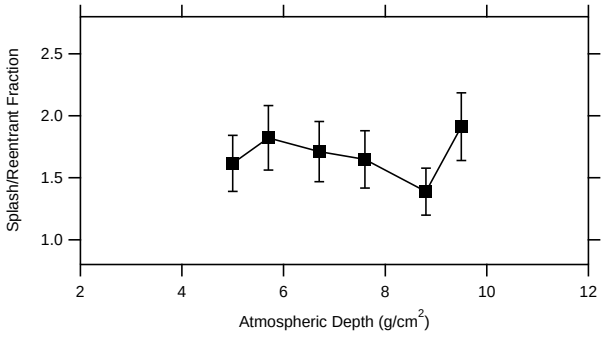

Fig. 4. The ratio of splash to reentrant albedo as a function of depth in the atmosphere. Splash albedo particles are expected to outnumber the downward-going counterparts simply because of propagation losses for the reentrant albedo.

HEAT measurements in the atmosphere and AMS measurements in low Earth orbit, new work in modeling the reentrant albedo is eagerly anticipated. The power-law spectrum of $E^{-1.6}$ on Figure 2 is to guide the eye since the spectrum involves the convolution of the primary ($E^{-2.7}$) spectrum with the high-P_T secondary production process, propagation back to the ToA, propagation to the other hemisphere, and then propagation down to the observed atmospheric depth.

3.2 Splash electron albedo

The splash albedo, in contrast to the reentrant albedo, is straightforward to measure with no significant backgrounds. All upward-moving electrons are included in our splash electron albedo measurement. The secondary nature of both albedo populations is clear in Figure 3, with the combined splash and reentrant electron albedo population being approximately half positrons. Both splash and reentrant albedo populations individually are consistent with a positron fraction of 0.5.

The number of splash electrons at all atmospheric depths (see Figure 4) is greater than the number of reentrant electrons at the same depth. In essence, this is due to the relatively local origin of the splash population and the much more significant propagation losses for the reentrant particles. A detailed simulation would be necessary to fully model